LARGE DEFLECTION ELASTIC-PLASTIC ANALYSE OF BEAMS, COLUMNS AND ARCHES

SUHARA, Jiro
Faculty of Engineering, Kyushu University: Professor

FUKUDA, Jyunko
Faculty of Engineering, Kyushu University: Research Assistant

https://doi.org/10.5109/7173518

出版情報：Reports of Research Institute for Applied Mechanics. 23 (72), pp.61-83, 1975. 九州大学応用力学研究所
バージョン：

Reports of Research Institute for Applied Mechanics
Vol. XXIII, No. 72, 1975

LARGE DEFLECTION ELASTIC-PLASTIC ANALYSES OF BEAMS, COLUMNS AND ARCHES

By

Jiro SUHARA* and Jyunko FUKUDA**

A numerical method of analyses for elastic-plastic bending and axial loading of beams, columns and arches taking into account of large deflection and material non-linearity is presented. The governing equations cover classical elastica problem, snap-through buckling of arches and large deflection analysis of beam-columns and so on assuming of stress-strain relations of any type. Predictor-corrector method and iterations are used to secure good accuracy of the solutions. Many examples are shown to prove the wide applicability and accuracy of the proposed method comparing to correspooding specific solutions already presented by various investigators.

I. Introduction

The analytical treatment of elastic bending of thin bars taking into account of large deflection is well known as the elastica problem. Oden and Childs[1] in 1970 and Monasa[2] in 1974 treated similar problems assuming a specific moment-curvature relations expressing elastic-plastic bending of bars approximately and Löbel[3] and Huddleston[4][5] also treated large elastic deflections of circular arches. These theories were based on linear or nonlinear elasticity or plasticity of specific types of the materials and neglecting the effect of axial deformation. On the other hand the finite extensional deformation of a rigid-perfectly plastic arch was treated by DaDeppo and Schmidt[6]. Authors present a method of analyzing the bending and the stretching of linear or curved uniform bars considering finite elastic or elastic-plastic deformations based on Bernoulli-Euler assumption and an elastic or an elastic-plastic stress-strain law of any type but neglecting the effect of shearing strain. As well the elastic or elastic-plastic stability of beams and arches as the effect of membrane force for elastic or elastic-plastic bending of straight beams subjected to lateral load are treated in a unified way by the proposed method of numerical analysis. The numerical integration by means of predictor-corrector and iteration methods are used through out.

* Professor, Faculty of Engineering, Kyushu University.
** Research Assistant, Faculty of Engineering, Kyushu University.

II. Theory

Figure 1 shows the undeformed and the deformed center line of a curved cantilever arch of an arbitrary form loaded by concentrated forces P and Q in horizontal and vertical directions respectively at the point C' of distance F from the end of arch C. The bar CC' is vertical to the deformed center line of the arch at C and assumed to be rigid. The deformed arch is subjected to a distributed load p per unit length of the deformed arc at any point B being perpendicular to the deformed center line of the arch. We select a system of rectangular coordinates xoy, and ox and oy are axes in horizontal and vertical directions respectively as shown in figure 1 and putting the origin O at the fixed end of the arch. Any point A_0 on the undeformed center line of the arch is specified by arc length S measured from the point O along the undeformed arc and the corresponding point A at the deformed arch is specified by arc length S^* measured from O along the deformed arc of the arch and the point B which corresponds the point B_0 of the undeformed arch is specified by arc length $S^{*\prime}$ of the deformed arch, C corresponds C_0 in the deformed and the undeformed center lines respectively. Coordinates of those points referred to xoy axes and the positive directions of bending moment and axial force are as shown in figure 1. Other important geometric quantities are the inclinations θ_0, θ, θ' and θ_c of the final tangents at O, A, B and C respectively.

Then the bending moment and axial force at any point A of the deformed arch are given as follows.

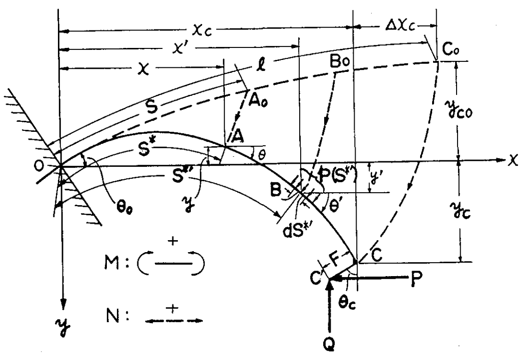

Fig. 1. Geometry and forces.

$$
\begin{aligned}
M(S^*) &= -P(y_c-y)+Q(x_c-x)+M_c \\
&\quad -\int_A^C p(S^{*\prime})(y'-y)\sin\theta'\,dS^{*\prime}-\int_A^C p(S^{*\prime})(x'-x)\cos\theta'\,dS^{*\prime} \\
N(S^*) &= -P\cos\theta-Q\sin\theta \\
&\quad -\left(\int_A^C p(S^{*\prime})\sin\theta'\,dS^{*\prime}\right)\cos\theta+\left(\int_A^C p(S^{*\prime})\cos\theta'\,dS^{*\prime}\right)\sin\theta
\end{aligned}
\tag{1}
$$

where

$$\frac{dx'}{dS^{*\prime}}=\cos\theta'] \quad \frac{dy'}{dS^{*\prime}}=\sin\theta'$$

Denoting the axial strain of the arch at any point A by $\varepsilon_m(S)$ as a function of the undeformed arc length of the corresponding point A_0 (tensile strain is assumed as positive) the deformed arc length S^* for a point A is given by

$$S^*=\int_0^S\{1+\varepsilon_m(S)\}dS$$

Treating a curved bar of uniform rectangular cross section of width b and depth $2h$ as an example, we describe above mentioned quantities in following non-dimensional forms, provided that ε_e is the yield strain of the material, σ_e the yield stress, N_e the yield axial force when no bending moment is applied, M_e the yield bending moment when no axial force is applied, M_0 the end moment of force applied at point O, I the geometric moment of inertia of the cross section, E the Young's modulus, E_p the plastic stress-strain rate, ρ_e the radius of curvature at the beginning of yielding and applying no axial strain, ρ^* the radius of curvature of the deformed center line, l the total undeformed arc length AC_0 $(L\equiv 2l)$, b' the rise of arch, R_0 the initial radius of curvature, 2α the included angle of circular arch and Δy the central deflection of the arch:

$$\xi=\frac{x}{l}, \quad \xi_c=\frac{x_c}{l}, \quad \xi'=\frac{x'}{l}, \quad \Delta\xi_c=\frac{(l-x_c)}{l}, \quad \beta=\frac{R_0\alpha^2\sqrt{A}}{\sqrt{I}}$$

$$s=\frac{S}{l}, \quad s'=\frac{S'}{l}, \quad s^*=\frac{S^*}{l}, \quad s^{*\prime}=\frac{S^{*\prime}}{l}, \quad \delta=\frac{\Delta y}{b'}$$

$$\eta=\frac{y}{y_0}, \quad \eta_c=\frac{y_c}{y_0}, \quad \eta'=\frac{y'}{y_0}, \quad y_0\equiv\frac{\varepsilon_e l^2}{h}, \quad \zeta=\frac{z}{h}$$

$$\mathfrak{M}(s)=\frac{M(S)}{M_e}=\frac{M(S)h}{\sigma_e I}=\frac{3M(S)}{2bh^2\sigma_e}, \quad \text{ⓜ}=\frac{M_0}{M_e} \tag{2}$$

$$\mathfrak{M}_c(s)=\frac{M_c(S)}{M_e}\equiv\mathfrak{M}(1)-c(k^2{}_0\cos\theta_c+j^2{}_0\sin\theta_c), \quad c\equiv\frac{F}{y_0}=\frac{Fh}{\varepsilon_e l^2}$$

$$\mathfrak{N}(s)=\frac{N(S)}{N_e}=\frac{N}{2bh\sigma_e}, \quad \mathfrak{N}(1)=\mathfrak{N}_c, \quad \mathfrak{N}(0)=\mathfrak{N}_0$$

$$k_0{}^2=\frac{Pl^2}{EI}, \quad j_0{}^2=\frac{Ql^2}{EI}, \quad m=\frac{p_0l^2}{2M_e}=\frac{3p_0l^2}{4bh^2\sigma_e}$$

$$\Omega=\frac{y_0}{l}=\frac{\varepsilon_e l}{h}, \quad \kappa^*=-\frac{\rho_e}{\rho^*}=-\frac{h}{\varepsilon_e\rho^*}, \quad \lambda=\frac{h}{l},$$

Assuming simply that the distributed load is uniform and applied perpendicularly to the deformed center line of the arch, then we have non-dimensional form of equations (1) as follows:

$$\mathfrak{M}(s) = -k_0^2(\eta_c-\eta)+\frac{j_0^2}{\Omega}(\xi_c-\xi)+\mathfrak{M}_c-m\left\{(\xi_c-\xi)^2+\Omega^2(\eta_c-\eta)^2\right\}$$

$$= \textcircled{m}+k_0^2\eta+\frac{j_0^2}{\Omega}(\xi_0-\xi)-m\left\{(\xi_0-\xi)(2\xi_c-\xi_0-\xi)-\Omega^2\eta(2\eta_c-\eta)\right\} \tag{3}$$

$$\textcircled{m} = -k_0^2\eta_c+\frac{j_0^2}{\Omega}(\xi_c-\xi_0)+\mathfrak{M}_c-m\left\{(\xi_c-\xi_0)^2+\Omega^2\eta_c^2\right\}$$

$$\mathfrak{N}(s) = -\frac{\lambda}{3\Omega}(k_0^2\cos\theta+j_0^2\sin\theta)-\frac{2m}{3}\left\{\varepsilon_e(\eta_c-\eta)\cos\theta-\lambda(\xi_c-\xi)\sin\theta\right\}$$

where ξ_0 is the non-dimensional abscissa of the end point O.†

The curvature κ^{*}†† of the deformed center line at any point A is given by

$$\frac{1}{\rho^*}=\frac{d\theta}{dS^*}$$

Then we have

$$\kappa^* = -\frac{\lambda}{\varepsilon_e}\cdot\frac{d\theta}{ds^*} = -\frac{\lambda}{\varepsilon_e}\cdot\frac{1}{1+\varepsilon_m}\cdot\frac{d\theta}{ds} \tag{4}$$

Let z axis be perpendicular to the undeformed and the deformed center lines of the arch passing through the corresponding points before and after deformation respectively, the fiber strain component being parrallel to the deformed and the undeformed center lines be $\varepsilon(z, S)$ or using non-dimensional coordinates ζ and s, $\varepsilon(\zeta, s)$ and the corresponding fiber stress be $\sigma(z, S)$ or $f(\zeta, s)=\sigma(z, S)/\sigma_e$ in non-dimensional form, where the stress-strain relation is given as $f(\zeta, s)=f[\varepsilon(\zeta, s)/\varepsilon_e]$. We denote $f(\zeta)$ for $f(\zeta, s)$ and $\kappa_0(s)$ for non-dimensional initial curvature simply. Then according to Bernoulli-Euler assumption, we have

$$\varepsilon(\zeta) = \left\{(1+\varepsilon_m)\kappa^*-\kappa_0\right\}\varepsilon_e\zeta+\varepsilon_m \tag{5}$$

Then we get non-dimensional bending moment and axial force as follows:

$$\begin{aligned}\mathfrak{N}(s) &= \frac{1}{2}\int_{-1}^{1} f\left[\left\{(1+\varepsilon_m)\kappa^*-\kappa_0\right\}\zeta+\frac{\varepsilon_m}{\varepsilon_e}\right]d\zeta\\ \mathfrak{M}(s) &= \frac{3}{2}\int_{-1}^{1} f\left[\left\{(1+\varepsilon_m)\kappa^*-\kappa_0\right\}\zeta+\frac{\varepsilon_m}{\varepsilon_e}\right]\zeta d\zeta\end{aligned} \tag{6}$$

where f is the function of strain $\varepsilon(\zeta, s)$ of arbitrary form given by experimental result†††. However we use simply the bilinear law shown in figure 2 in the following analyses, for which the strain hardning factor is taken 1/30 or 1/50 as shown in following figures.

† It is assumed that ξ_0 is equal to 0 in figure 1.

†† "*" means "considering the effect of axial strain" for the corresponding quantity in the following.

††† For instance, we can use the elastic-plastic stress-strain relation for steel subjected to repeated load beyond elastic limit[7].

III. Numerical Solutions

For a simple cantilever arch type problem, giving the initial form or the given

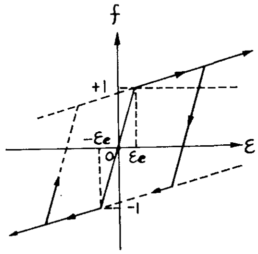

Fig. 2. Bilinear stress-strain law.

deformed form of the curved center line of the arch, the curvature κ^* and the axial strain ε_m at the center of any section A of the arch are obtained by iteration procedure giving $\mathfrak{N}(s)$ and $\mathfrak{M}(s)$ by equations (3) and $f(\varepsilon)$ and performing numerical integrations with respect to ζ for given plasticity law or analytical integration for bilinear or exponent type plasticity law in equations (6). Then we can obtain the coordinates of the deformed center line and the slope of the arch at any point by the predictor-corrector numerical integration method applied to equations (7) with respect to s and with desirable accuracy (refer to figure 3).

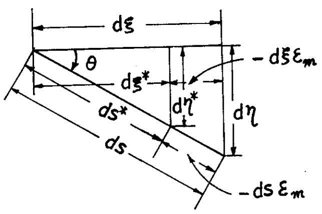

Fig. 3. Arc elememt of deformed arch.

$$\frac{d\xi^*}{ds} = (1+\varepsilon_m)\cos\theta\ , \quad \frac{d\eta^*}{ds} = \frac{1}{\Omega}(1+\varepsilon_m)\sin\theta\ , \quad \frac{d\theta}{ds} = -\frac{\varepsilon_e}{\lambda}(1+\varepsilon_m)\kappa^* \tag{7}$$

where

$$ds^* = (1+\varepsilon_m)ds$$

The iteration is continued until the obtained coordinates of any point of the deformed center line are unchanged for corresponding initial coordinates. Multiple iterations are necessary for highly indeterminate structures like both ends clamped arch or continuous beams. Table 1 shows the flow diagram for obtaining the solution of a uniformely loaded clamped arch problem.

Table 1. Flow chart of solving both ends clamped uniformly loaded beam or arch problem.

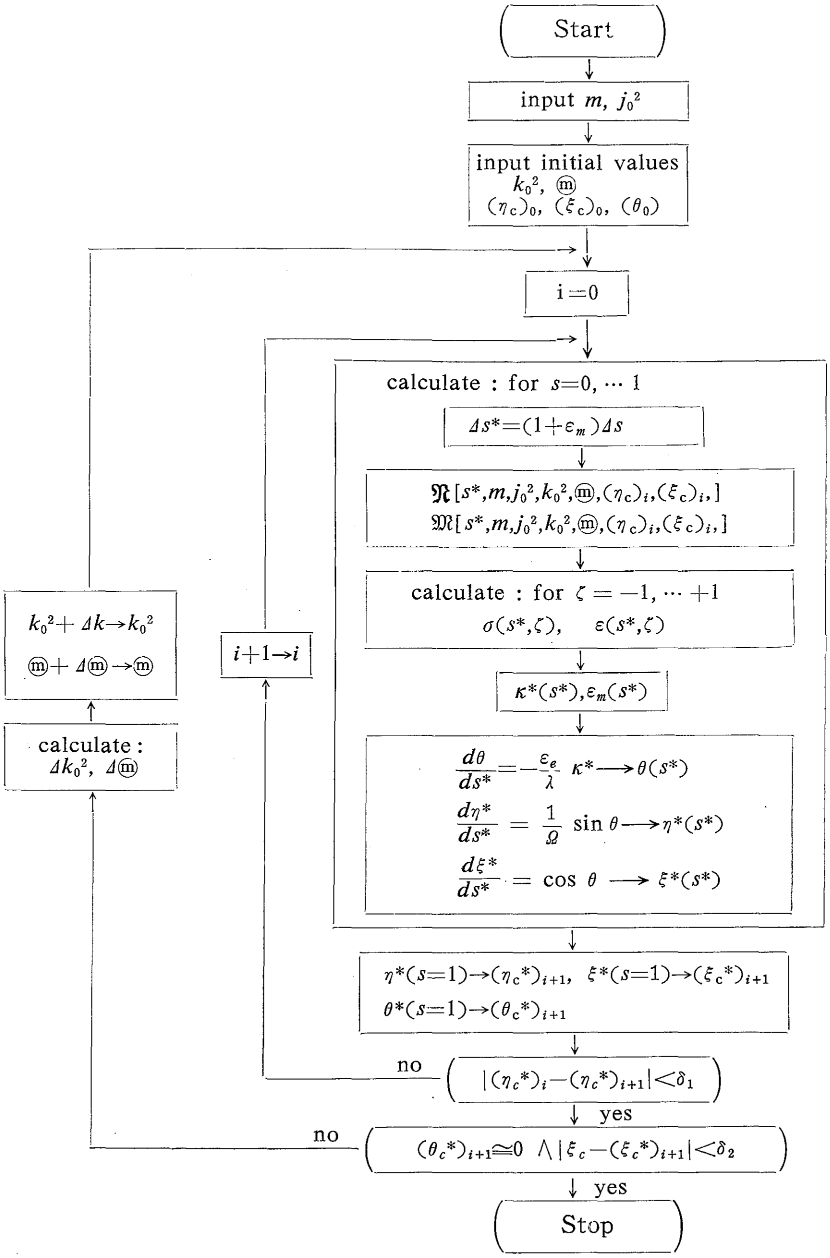

IV. Examples

(1) Cantilever beams

Bisshopp and Drucker[8] obtained an analytical solution of a large deflection problem of a cantilever beam subjected to a concentrated load vertically at a free end by using elliptic integrals.

Applying the authors' method to this problem, a single loop for integration procedure with respect to s is necessary to determine the abscissa ξ_c of the end of the beam, though it is assumed that ξ_c is unchanged therefore no iteration is necessary for the small deflection theory. Figure 4 shows very good agreements between both results of the analytical method and the present method for changes of coordinates ξ_c and y/l of the free end of the cantilever beam which undergoes large deflection. And the figure also shows the elastic-plastic deflection obtained by the present method which can not be obtained by the Bisshopp and Drucker's method. The deflection patterns for various tip loads are shown in figure 5 comparing elastic and plastic ones.

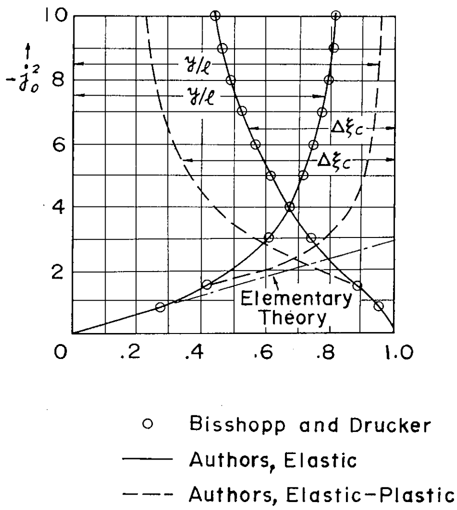

Fig. 4. Load versus vertical and horizontal displacements at the end of a cantilever beam.

(2) Elastica and Plastica problems

The large deflection problem of a slender straight column subjected to a vertical axial load without initial eccentricity is well known as the elastica problem[9]. Comparisons were made between the analytical solution and the present numerical one. No discrepancy is found practically between them as shown in figure 6 and figure 7.

The solution of elastic-plastic deflection (to be called plastica-problem) of

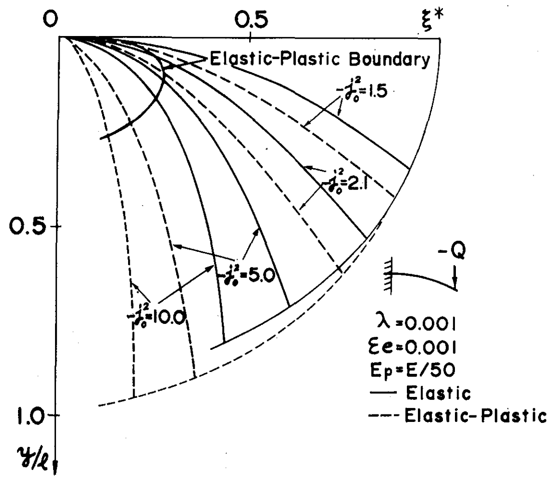

Fig. 5. Deflection curves of a cantilever beam for various end loads.

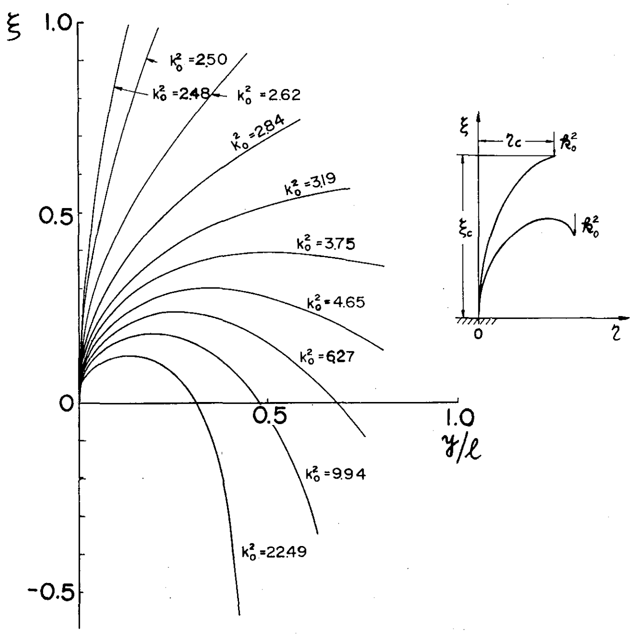

Fig. 6. Deflection curves of a column for various vertical loads.

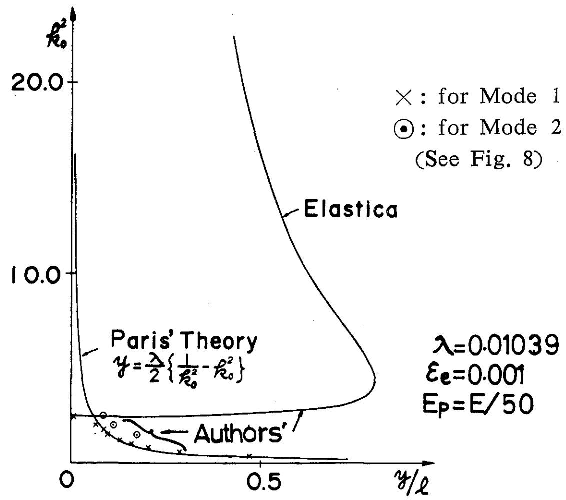

Fig. 7. Vertical load versus maximum deflection curves.

the same problem obtained by the present method are shown in figure 7 and figure 8. In the figure 8, the fundamental and the second elastic-plastic large deflection modes are shown where the thickness length ratio is exaggerated.

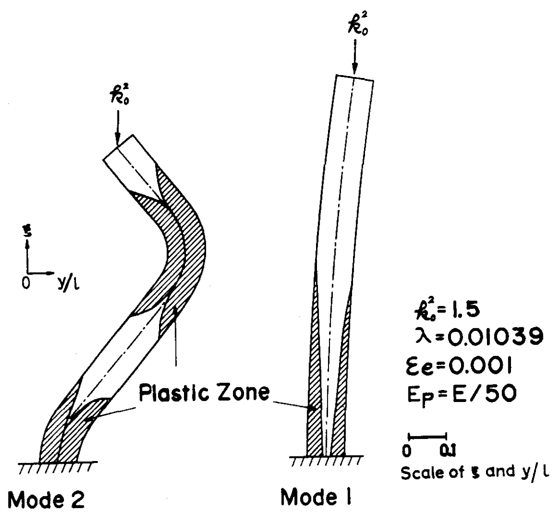

Fig. 8. Large elastic-plastic deflection modes for a column

For the cases of relatively short steel column, plastic buckling should be considered, consequently the large deflection analysis is necessary for analyzing large plastic deflection after the formation of plastic region, the present method can also cover such cases.

Examples treated by Paris[10] assuming the concept of limit analysis for elastic-ideal plastic materials giving the relations between loads, vertical displacements and maximum deflections of straight columns are shown in from figure 9 to figure 14 comparing results obtained by the present method assuming a elastic-linear strain hardening law (strain hardening rate is assumed to be 1/30 of elastic modulus) together with showing residual stress distributions of critical

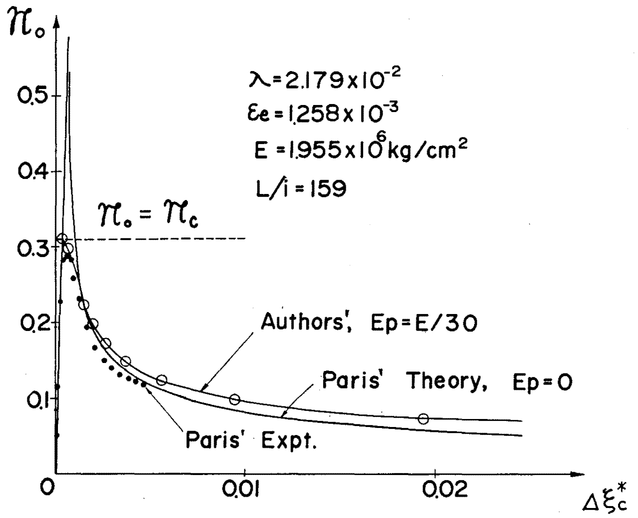

Fig. 9. Vertical load versus vertical displacement for a column

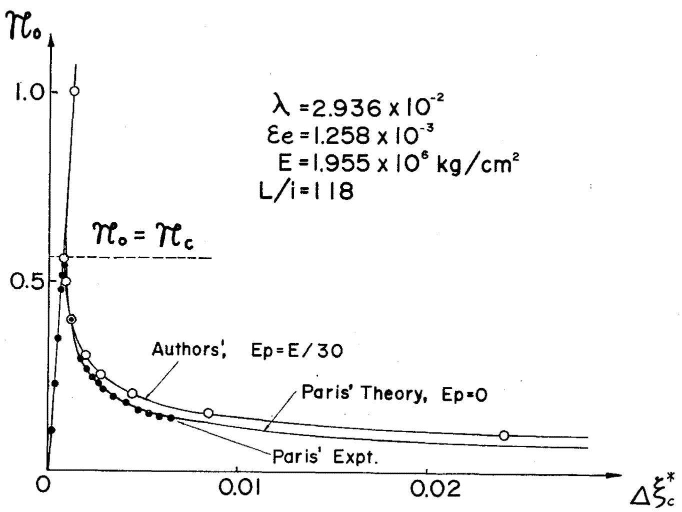

Fig. 10. Vertical load versus vertical displacement for a column

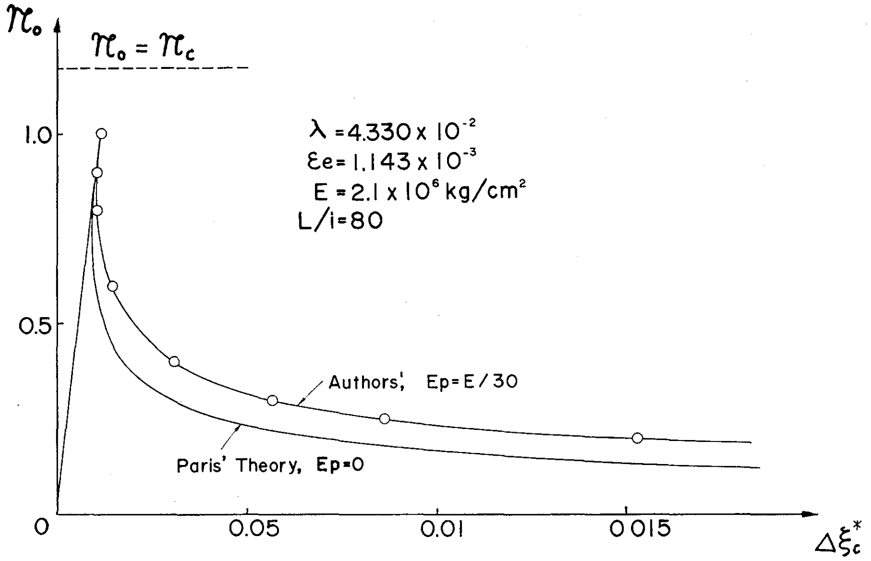

Fig. 11. Vertical load versus vertical displacement for a column

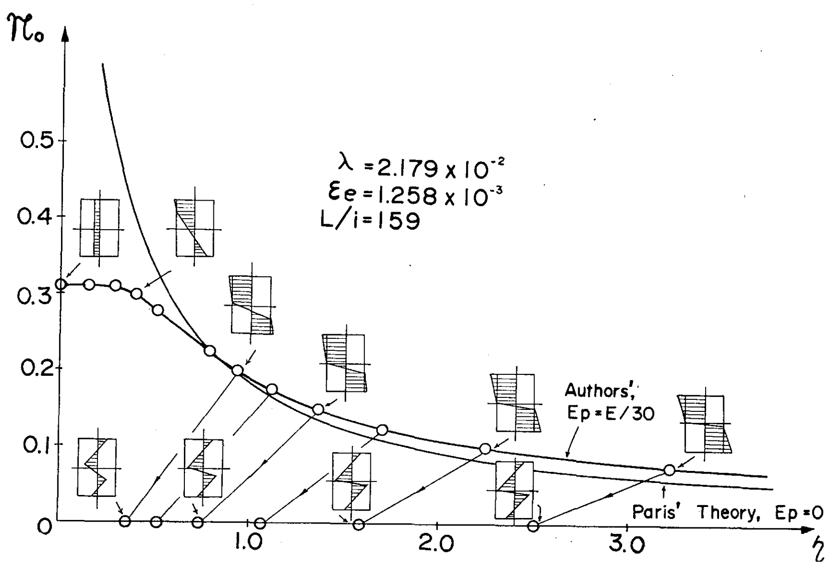

Fig. 12. Vertical load versus maximum deflection curves and stress distributions of critical section for a column.

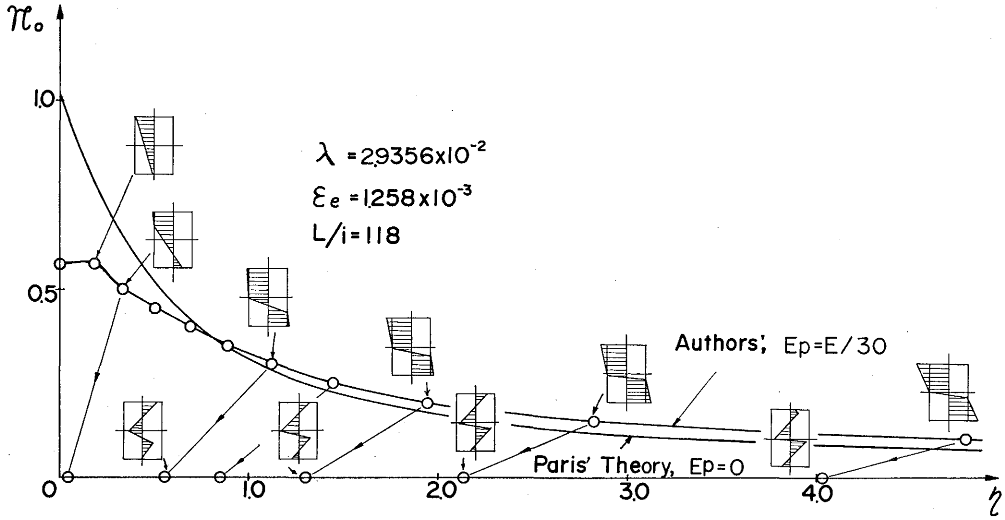

Fig. 13. Vertical load versus maximum deflection curves and stress distributions of critical section for a column.

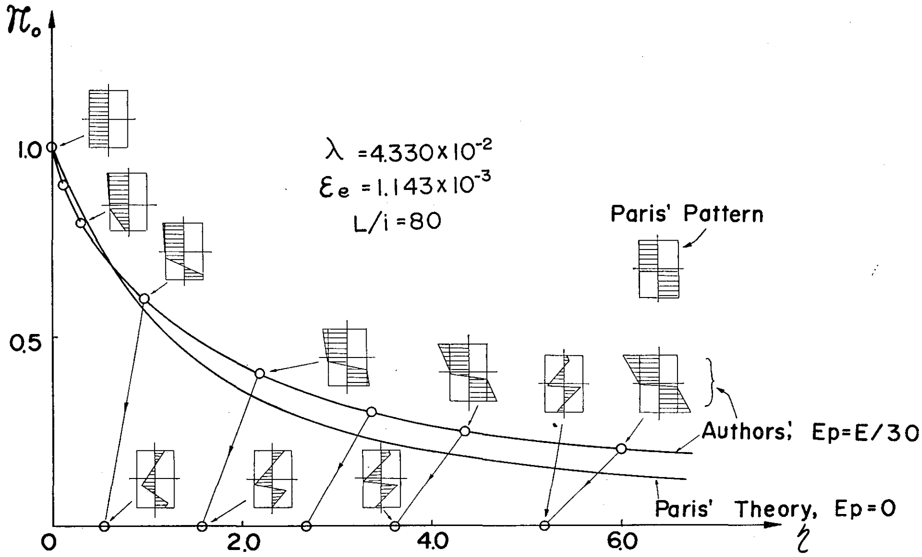

Fig. 14. Vertical load versus maximum deflection curves and stress distributions of critical section for a column.

sections after unloading by providing the subroutine of calculating strain reversal. The maximum strain to be able to judge whether it exceeds ultimate strain or not can be obtained by the present method, whereas it is impossible to obtain by the method of the limit analysis. Good agreements between the results by both methods are obtained for estimating initial palstic buckling behaviour, but slight discrepancies are found in post buckled behaviour which are considered as mainly due to the difference of stress-strain law beyond elastic limit. Figure 15 shows the effect of initial eccentricity of axial load applied to a straight steel column illustrating the load versus maximum deflection characteristics. The results obtained by the authors' method agree with the results by a finite element method presented by Fujita *et al.*[11], as well those by a plastic hinge method proposed by one of the authors *et al.*[12].

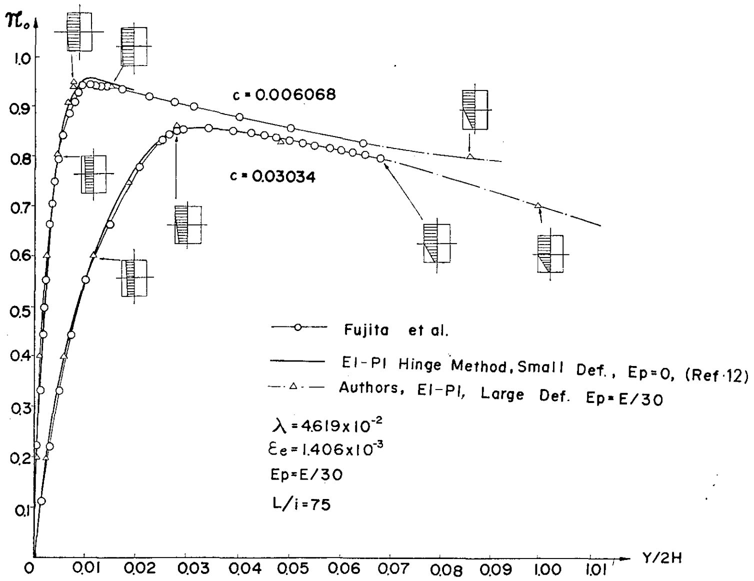

Fig. 15. Vertical load versus deflection curves for a eccentrically loaded column.

Figure 16 and figure 17 show the elastic-plastic deflections of straight beams subjected to bending and axial force, providing that the former is the case lateral load being proportional to axial load whereas the latter is the one being axial force kept constant.

The results show that the elastic-plastic hinge method based on small deflection theory is valid to estimate approximate collapse loads in these examples but the behaviour beyond the collapse load depends upon the plastic stress-strain rate.

(3) Steel strip subjected to hydrostatic pressure and membrane stress.

Young[13] calculated the deflection of initially straight steel strip subjected to hydrostatic pressure by use of plastic hinges and taking into account of membrane action and showed good agreement between deflections for various loads

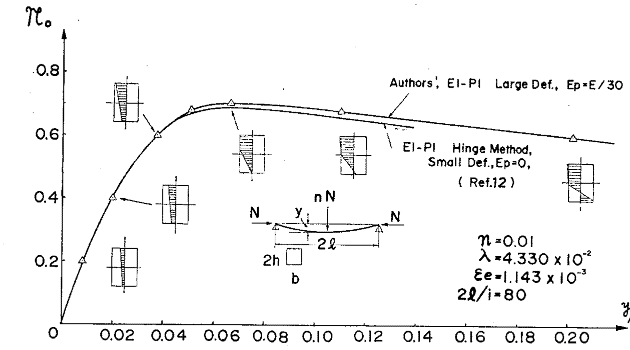

Fig. 16. Load versus deflection curves for a beam-column subjected to proportionally increasing lateral and axial loads.

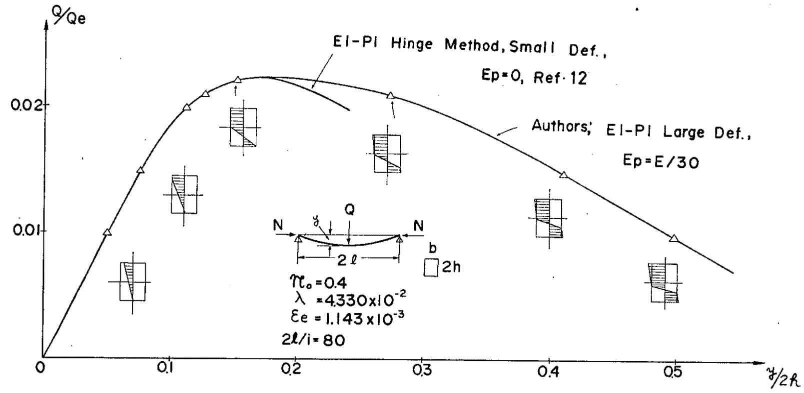

Fig. 17. Load versus deflection curves for a beam-column subjected to increasing lateral and constant axial loads.

obtained by theory and experiment respectively. However this theory can not afford the exact strain distributions, as well as neither the residual stress nor residual deflection. The deflecetions obtained by authors' results assuming the elastic-linear strain hardening law ($E_p=E/50$) and exact fixing conditions at both ends, agree fairly with those by both Young's theory and experiments as shown in figure 18 and the authors' method can give all of the above mentioned quantities simultaneously.

(4) Snap through buckling of arches

Kerr and El-Bayoumy[14] treated the elastic snap through buckling problem of a shallow arch clamped at both ends and subjected to a uniform lateral load by using the exact solution of nonlinear governing equation. A comparison of the load-deflection curves of the case of $R_0\alpha^2/2h=6$ was made for the load-deflection curves obtained by Kerr anh El-Bayoumy's by the authors' method. Satis-

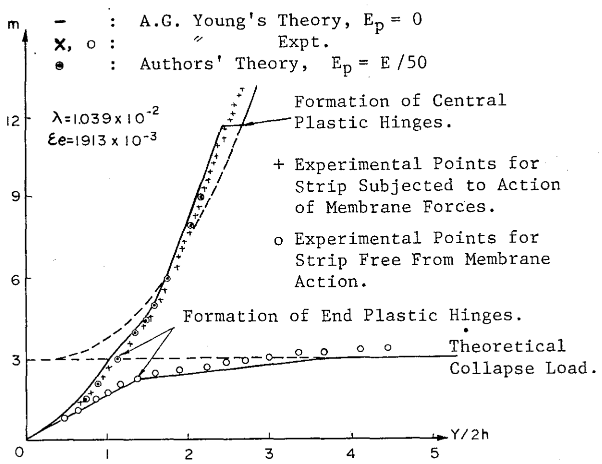

Fig. 18. Load versus deflection curves for both ends fixed and freely supported hydrostatically loaded strips.

factory agreement was certified for elastic snap through characteristics. The results shown in following examples are obtaiend by the authors' method including the capability of treating elastic-plastic analyses of the circular arches assuming symmetrical deflections.

Figure 19 shows elastic load-deflection characteristics of circular arches clamped at both ends subjected to a concentrated load at the midle point of the span for various configurations of the arches and figures 20, 21, 22 and 23 show comparisons of elastic and elastic-plastic changes of central deflections, the forms of the deflections, the horizontal reactions at ends and the end moments respectively for various values of loads $-j_0^2$ and the ratio of thickness to total arc length λ but including angle 2α is kept constant. And figures 24 and 25 show the changes of deflection and horizontal reactions due to the variation of a concentrated load for both end pinned circular arches.

Figures 26, 27 and 28 show the variations of the deflections, the horizontal reactions and end moments of hydrostatically loaded circular arches clamped at both ends. And figures 29 and 30 show the variations of deflection and the horizontal reaction of hydrostatically loaded pinned arch. It is recognized that the effects of plasticity upon the snap through buckling phenomena are great for every cases mentioned above.

V. Discussions

The shooting method together with numerical integration along the deformed axis is used through out to determine the statically indeterminate quantities, i.e., the horizontal displacement at free end for the case of the large deflection of cantilever beam, the maximum deflection for the case of elastica and plastica

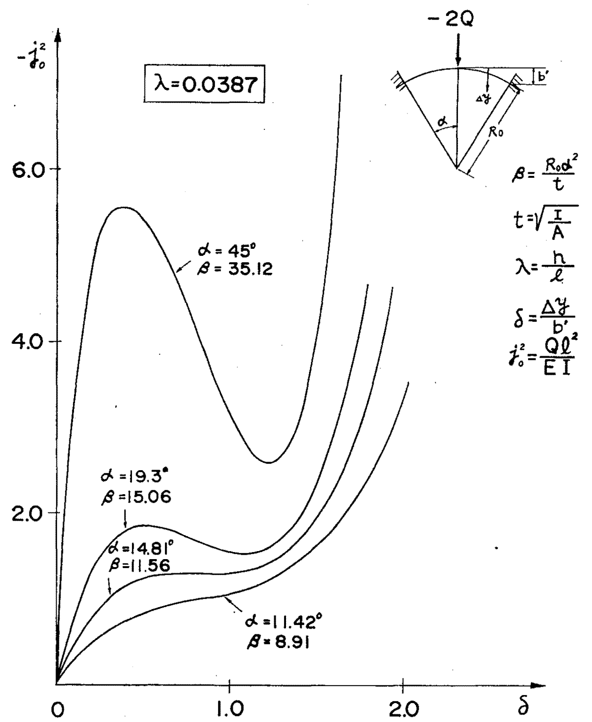

Fig. 19. Load versus elastic central deflection curves for arches of various configurations.

problems, the moment of force at the clamped end and the axial force at the center of the arch for the case of both end clamped circular arch subjected to a concentrated load, the central deflection in addition for the case of hydrostatically loaded arch and finally axial force at the center of the arch and the central deflection are indeterminate quantities for the both end pinned arch according to equations (3).

Good accuracy of the results is obtained by these methods for above mentioned examples, but computing time required to converge the solution is affected by initially assumed values of statically indeterminate quantities. In the above mentioned examples, stepwise and appropriately increased values of indeterminate quantities according to the increase of load are assumed as input values to minimize the computing time for each steps of loads by watching the curves of growth of the nonlinear changes of the indeterminate quantities according to the changes of external load. It is necessary to find automatically the optimum policy of estimating the initial values of statically indeterminate quantities in the next stage of this study.

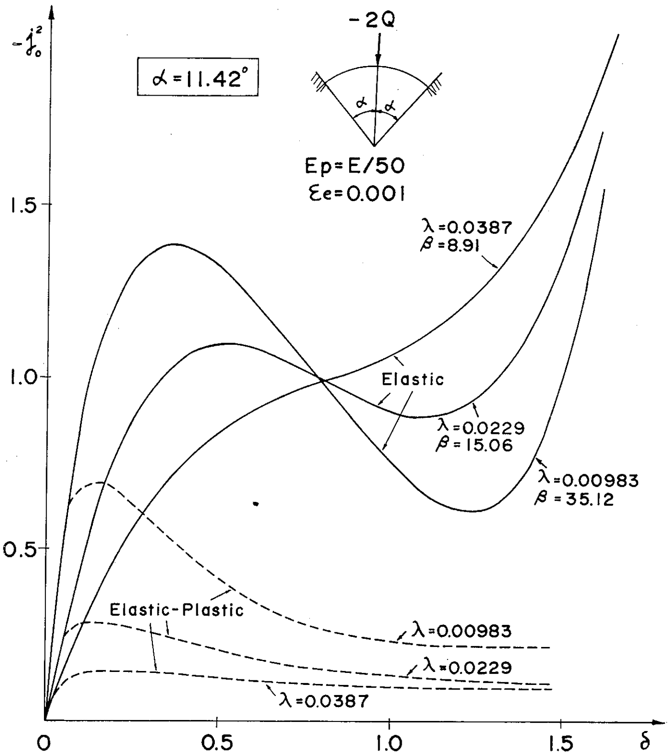

Fig. 20. Comparison of load versus elastic and elastic-plastic central deflection curves for arches.

VI. Conclusions

A method of analyzing the deformations of straight or curved bars taking into account of geometrical and material nonlinearity is presented and good accuracy of the obtained solutions and the wide applicability of the proposed method is proved by many examples. It is considered that the estimation of ultimate deformation or strength of assembly of one dimensional structures with more complexity like frame structures composed of the linear or curved memberes are become possible by application of the proposed method together with using actual stress-strain law of the material[7].

References

1) Oden, J. T. and Childs, S. B., Finite Deflections of a Nonlinearly Elastic Bar, Jour. Appl. Mech., March, 1970, pp. 48-52.

2) Monasa, F. E., Deflections and Stability Behavior of Elastic-Plastic Flexible Bars, Jour. Appl. Mech., June 1974, pp. 537-538.

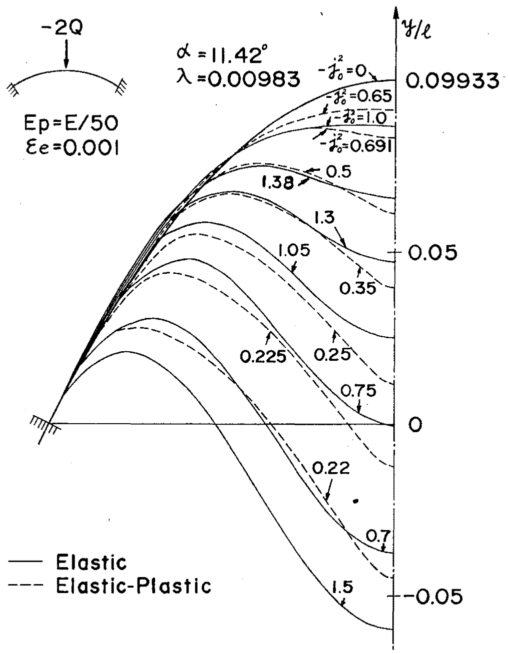

Fig. 21. Comparison of elastic and elastic-plastic deflections for a clamped arch for various values of load.

3) Löbel, von G., Grosse Biegeverformungen bei schlanken geraden und kreisformigen Trägern, Z. A. M. M. 43, Heft 1/2, 1963, Seite 25–46.
4) Huddleston, J. V., Finite Deflections and Snap-Through of High Circular Arches, Jour. Appl. Mech., Dec., 1968, pp. 763–769.
5) Huddleston, J. V., Behavior of a Steep Prestressed Arch Made from a Buckled Strut, Jour. Appl. Mech., Dec., 1970, pp. 984–994.
6) DaDeppo, D. A. and Schmidt, R., Finite Extensional Deformation of a Rigid Plastic Arch, Int. Jour. Solids Struct., Vol. 10, 1974, pp. 1017–1034.
7) Suhara, J., Shugyo, M., Fukuda, J. and Nagano, H., The Stress-Strain Behaviours of Mild Steel Under Complex Loading History, Rep. Res. Inst. Appl. Mech. Kyushu Univ., Vol. 23, No. 72, 1975.
8) Bisshopp, K. E and Drucker, D. C., Large Deflection of Cantilever Beams, Quart. Appl. Math. Vol. 3, 1945, pp. 272–276.
9) Timoshenko, S. P. and Gere, J. M., Theory of Elastic Stability, Mc-Graw-Hill, New York, 1961.
10) Paris, P. C., Limit Design of Columns, Jour. Aeron. Sci., Vol. 21, No. 1, 1954, pp. 43–49.
11) Fujita, Y., Ohotsubo, H. and Yuhara, T., Plastic Design of Steel Structure (11th Rep.),
—— Maximum Strength of Framed Structure —— (in Japanese), Jour. Soc. Nav. Arch. Japan, Vol. 129, 1971, pp. 203–211.
12) Suhara, J. and Nagano, H., The Strength Analysis of Framed Structures by Means

ERRATUM: Change Figure 25 for Figure 30 each other.

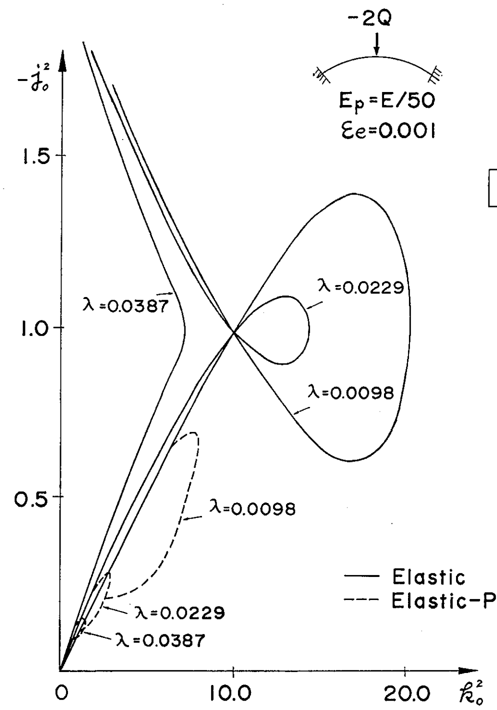

Fig. 22. Load versus horizontal end reaction curves for clamped arches.

of Elasto-Plastic Hinge Method (in Japanese), Trans. West-Japan Soc. Nav. Arch., No. 45, 1973, pp. 211-230.

13) Young, A. G., Ship Plating Loaded Beyond the Elastic Limit, Trans. Inst. Nav. Arch., No. 2, Vol. 101, 1959, pp. 143-165.

14) Kerr, A. D. and El-Bayoumy, L., On the Nonunique Equilibrium States on a Shallow Arch Subjected to a Uniform Lateral Load, Quart. Appl. Math., Vol. 28, Oct., 1970, pp. 399-409.

(Received April 30, 1975)

(Figure 23~figure 30 are presented in succeeding pages.)

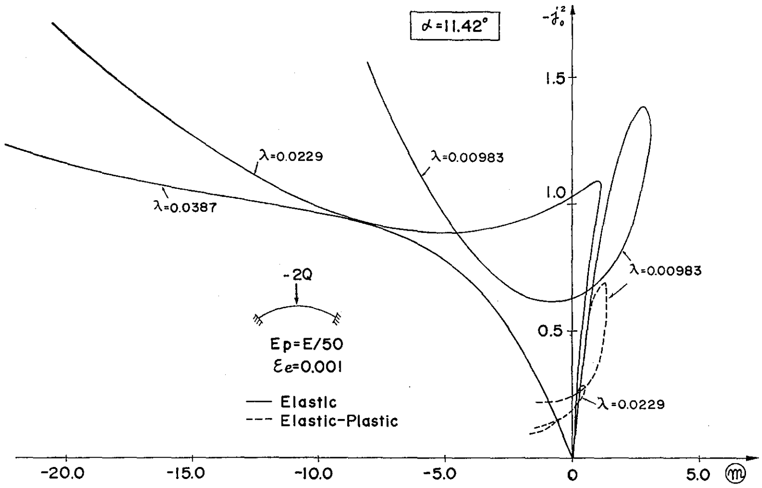

Fig. 23. Load versus end moment curves for clamped arches.

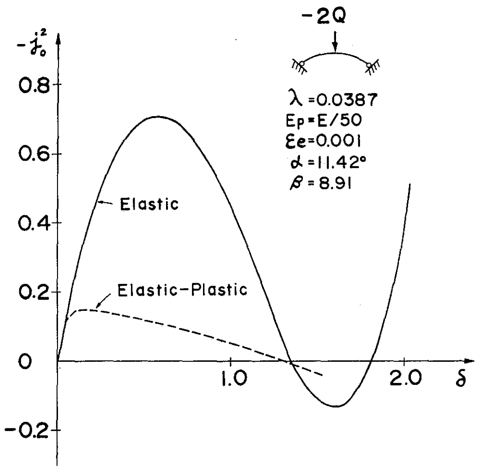

Fig. 24. Load versus central deflection curves for a pinned arch.

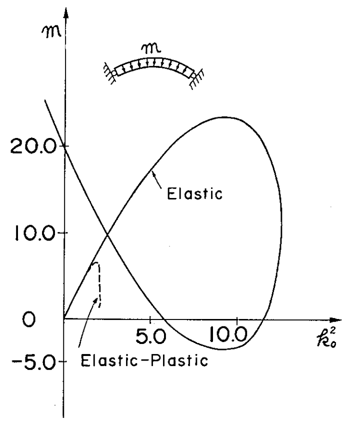

Fig. 25. Load versus horizontal end reaction curves for a pinned arch.

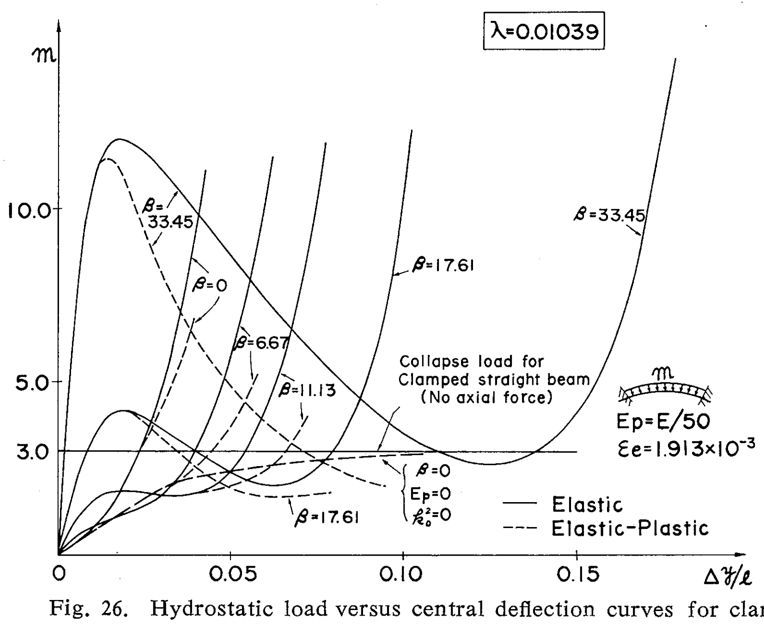

Fig. 26. Hydrostatic load versus central deflection curves for clamped arches.

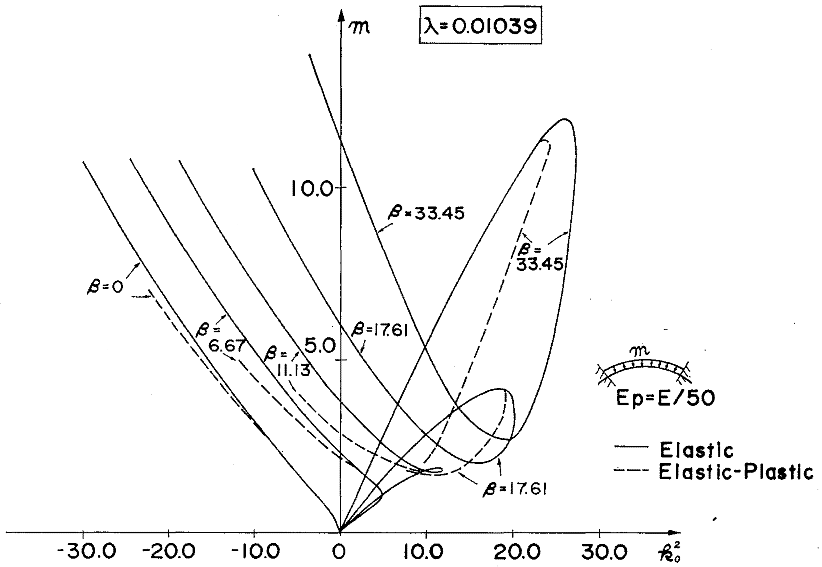

Fig. 27. Hydrostatic load versus horizontal end reaction curves for clamped arches.

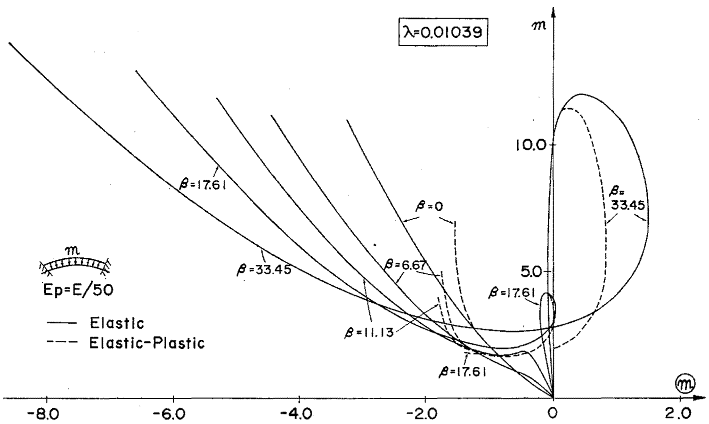

Fig. 28. Hydrostatic load versus end moment curves for clamped arches.

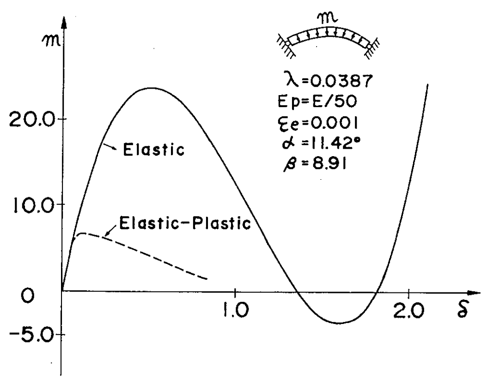

Fig. 29. Hydrostatic load versus deflection curves for a pinned arch.

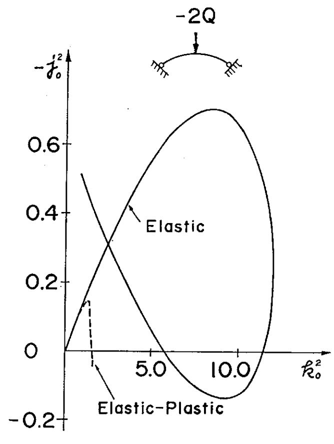

Fig. 30. Hydrostatic load versus horizontal end reaction curves for a pinned arch.